

Encephalization and allometric trajectories in the genus *Homo*: Evidence from the Neandertal and modern lineages

Emiliano Bruner^{*†}, Giorgio Manzi^{*†}, and Juan Luis Arsuaga[§]

^{*}Dipartimento di Biologia Animale e dell'Uomo, Università "La Sapienza," Piazzale Aldo Moro 5, 00185 Rome, Italy; [†]Istituto Italiano di Paleontologia Umana, Piazza Mincio 2, 00198 Rome, Italy; and [§]Unidad de Investigación Sobre la Evolución y Comportamiento Humano, Universidad Complutense, Instituto Carlos III, Calle Sinesio Delgado, 4 (Pb. 14), 28029 Madrid, Spain

Contributed by Juan Luis Arsuaga, October 14, 2003

The term "encephalization" is commonly used to describe an enlargement in brain size, considered as either absolute endocranial volumes or relative values in relation to body size. It is widely recognized that a considerable endocranial expansion occurred throughout the evolution of the genus *Homo*. This article aims to evaluate whether this phenomenon was the outcome of distinct evolutionary lineages, reaching similar brain expansions but through different trajectories. Endocranial morphology was studied in a sample of fossil hominines by multivariate approaches using both traditional metrics and geometric morphometrics. The analysis was focused on the transition from a generalized archaic pattern within the genus *Homo* to the modern morphology and compared with changes that occurred along the Neandertal lineage. The main result was the identification of two different evolutionary trajectories, in which a similar expansion in endocranial size has been reached by different changes in shape. Along the Neandertal lineage we observed maintenance of an "archaic" endocranial model, in which a large amount of variability is based on a single allometric trend. By contrast, when modern endocasts were compared with nonmodern ones, we found important differences apparently led by a parietal expansion. In this light, the origin of our species may have represented the opportunity to surpass the constraints imposed on encephalization by the ontogenetic pattern shared by nonmodern *Homo* representatives.

One of the most important questions in relation to the evolution of the genus *Homo*, and to the origin of *Homo sapiens*, is the nature of the evolutionary processes that were responsible for human encephalization (absolute and relative cerebral volumetric expansion) and the associated increase in behavioral complexity. Did human encephalization occur as the result of unilinear (i.e., anagenetic) evolution (1)? Alternatively, we argue that it may have occurred in distinct lineages within the genus *Homo* that evolved, in parallel, similar levels of brain expansion.

Furthermore, there is no clear evidence in relation to the pattern(s) involved. Various arguments have been put forward based on linear vs. exponential models of brain expansion involving gradual vs. discrete processes and regional vs. isolated population dynamics (e.g., refs. 2–6).

The elusive morphology of the brain and the extreme enlargement of the neocortex among the hominids make it difficult to describe and quantify its variability. This has always represented a limit for the paleoneurological approach, traditionally focused on the evaluation of the "cranial capacity," and sometimes to the description of single traits. In addition, the small number of fossil specimens useful for a paleoneurological approach, their fragmentary preservation, and the relatively meager knowledge we have on endocranial variation (as compared with ectocranial features) greatly limited the analysis in the past. Studies were usually limited to some of the most notable endocranial characters such as circumvolutions, asymmetries, and a few discrete traits (3). Despite the fact that several analyses produced valu-

able results, the descriptive nature of such an approach allowed only general conclusions, because "the information that we glean from endocasts remains (literally) superficial" (7). Moreover, when the endocranial traits have been considered separately, their fundamental relationships within the endocranial system as a whole, as well as with the structural network of the cranium itself (8), have been practically ignored. Recently, however, the analysis of endocranial surfaces can be carried out on a greatly enlarged fossil sample, and inferences on the evolution of the cephalic structures may be improved by more robust analytical support (9).

In this article, endocranial morphology is analyzed by means of multivariate morphometrics in a sample of fossil hominines, with special reference to the transition from a generalized archaic pattern within the genus *Homo* to the modern morphology of *H. sapiens*. To maximize our basis for interpretation and to approach the overall endocranial shape, methods used here include both traditional and geometric morphometrics (see ref. 10). The aim of our work is to identify those structural models that might be able to describe the principal pattern(s) involved in the evolution of the human brain. In particular, we have the opportunity to follow in some detail the changes that occurred in endocranial morphology among European populations from $\approx 400,000$ years before present (11) up to the Late Pleistocene. In addition to a rather large comparative sample of physical endocasts from specimens included in the *Homo erectus* hypodigm, as well as early modern and recent representatives of *H. sapiens*, our work is based on especially well preserved Middle Pleistocene fossils such as crania 4 and 5 from the Sima de los Huesos site of the Sierra de Atapuerca, Spain (SH4/5) (12, 13) and the recently described "virtual" endocast of the early Neandertal Saccopastore 1 (SCP1) from Italy (14, 15). These examples are especially appropriate to examine the Neandertal lineage, which represents a useful case study to investigate the occurrence in human brain evolution of a single sequence vs. more discrete events.

Materials and Methods

Metric variables and landmark data were collected on physical endocasts and from virtual reconstructions based on computed tomography and 3D image analysis (16, 17). Specimens were divided into three main groups according to their chronology, morphology, and evolutionary position. The first group includes individuals referred to as anatomically modern humans (MOD), and specimens assigned to the Neandertal variability have been fit into a second group (NDR). The third group includes more archaic specimens (ARC), representing individuals that are not

Abbreviations: SH4 and SH5, crania 4 and 5, respectively, from the Sima de los Huesos site of the Sierra de Atapuerca, Spain; SCP1, Saccopastore 1; PC, principal component.

[†]To whom correspondence should be addressed. E-mail: emiliano.bruner@uniroma1.it.

© 2003 by The National Academy of Sciences of the USA

Table 1. The sample, labels used, reference group, and repository place of the specimens

Specimen	Label	Group	Repository
Trinil 2	TRN2	ARC	BAU
Sangiran 2	SNG2	ARC	IPH
Salè	SAL	ARC	BAU
Sinanthropus III	ZKD3	ARC	BAU
Sinanthropus X	ZKD10	ARC	IPH
Sinanthropus XII	ZKD12	ARC	BAU
Arago (rec)	ARA	ARC	IsIPU
SH4	SH4	ARC	UC
SH5	SH5	ARC	UC
SCP1	SCP1	NDR	BAU
La Chapelle-aux-Saints	CHP	NDR	IsIPU
La Ferrassie 1	FRS	NDR	IPH
Teshik-Tash	TST	NDR	IPH
Guattari 1	GTT	NDR	IsIPU
Feldhofer Grotto	FLD	NDR	BAU
La Quina H5	QH5	NDR	IPH
Irhoud 1	IRH	—	IPH
Skhul V	SKH5	MOD	IPH
Predmosti 3	PRD3	MOD	IPH
Predmosti 4	PRD4	MOD	IPH
Predmosti 9	PRD9	MOD	IPH
Predmosti 10	PRD10	MOD	IPH
Combe-Capelle	CCP	MOD	BAU
Vestonice 2	VST2	MOD	IPH
Vatte di Zambana	VTT	MOD	IsIPU
Recent human endocast	RHE	MOD	IPH

BAU, Dipartimento di Biologia Animale e dell'Uomo (Rome); IPH, Institut de Paleontologie Humaine (Paris); IsIPU, Istituto Italiano di Paleontologia Umana (Rome); UC, Universidad Complutense (Madrid).

derived from either the modern or Neandertal morphotypes. Therefore, while the first two groups can be identified by specific (i.e., *H. sapiens* and *Homo neanderthalensis*, respectively) or

subspecific names, the latter group has no taxonomic value and includes humans ranging from the Early to the Middle Pleistocene on a large geographical scale (Asia, Africa, and Europe). Table 1 lists the entire sample, the labels used in the text and figures, the reference group, and the repository place of the specimens.

A set of metric variables has been taken on the endocasts (see Fig. 5, which is published as supporting information on the PNAS web site). In addition to absolute variables, relative values have been considered, such as the ratio between each diameter and the maximum hemispheric length (averaged hemispheres). These data have been used to calculate a principal components (PC) analysis, aimed at characterizing the variability in endocranial shape, and a cluster analysis (based on the Euclidean distance matrix and the unweighted pair-group method using arithmetic averages procedure) to assess the phenetic similarities. Cluster analysis was performed by using the Phylogeny Inference package [PHYLIP 3.57c (18)], and phenograms were computed with TREEVIEW (19).

In addition, 3D landmark coordinates have been collected on each physical endocast with a Microscribe 3DX or by means of dedicated software on the virtual reconstructions (3DVIEW and MAGIC COMMUNICATOR) of the SH4/5 and SCP1. Preliminary tests showed a correct correspondence between physical and virtual replicas. The resulting geometric model is a bilateral configuration based on a set of 23 landmarks (see Fig. 6, which is published as supporting information on the PNAS web site). The average shape for each group was calculated to compare the archaic model with the derived morphotypes in pairwise comparisons. The averaging procedure limits individual variability or asymmetry; however, the small sample size does not allow a full statistical analysis of the group-specific variation, and the result must be interpreted simply as a geometric comparison. Average shapes and comparisons were calculated by using MORPHEUS ET AL. (20). A PC analysis was performed on a reduced configuration, selected to increase the sample size and discard highly variable and “fuzzy” landmarks (21) such as the temporoparietal

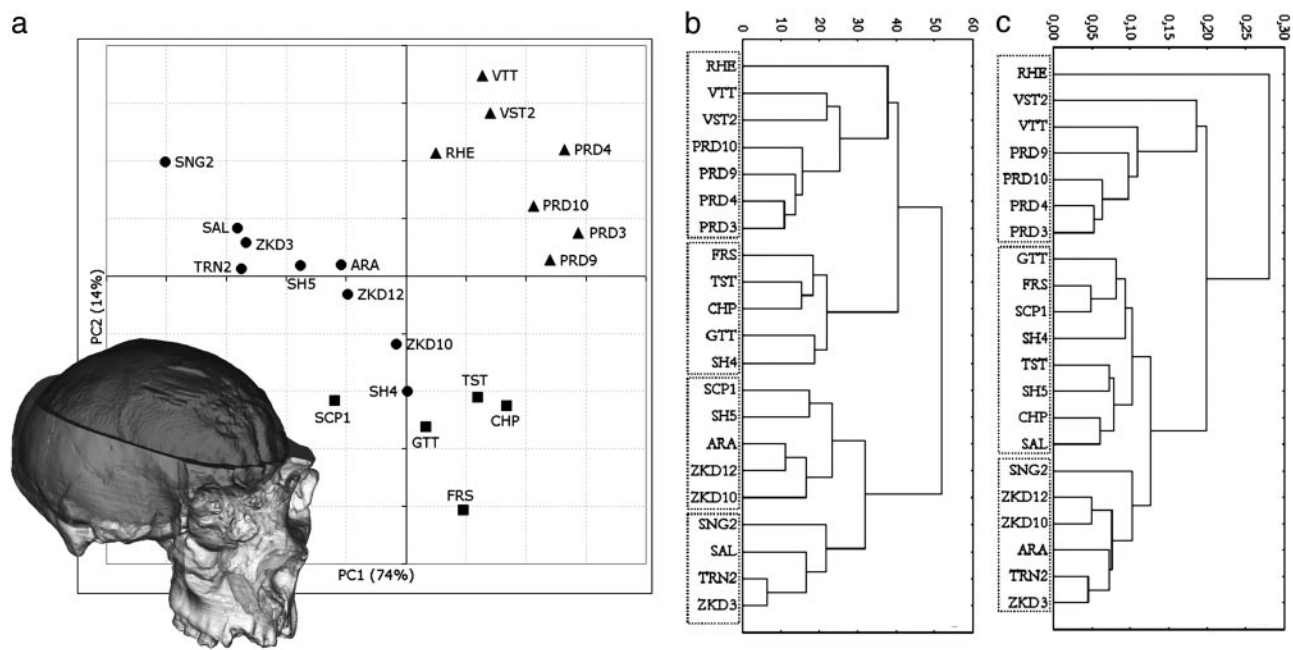


Fig. 1. The virtual reconstruction of the cranium and endocast of SCP1 is shown together with the plot of the first two PCs computed on nine metric variables taken on the endocasts (a) (see Fig. 5) and the unweighted pair-group method using arithmetic averages procedure cluster analysis based on the Euclidean distance matrices obtained from the absolute values (b) and the relative values (c). Cophenetic correlation coefficients are 0.74 and 0.85, respectively. ●, archaic specimens; ■, Neandertals; ▲, modern humans.

width or the supramarginal gyrus, which may represent a bias for the interpretation of individual specimens. Therefore, only part of the landmarks of the upper portion of the endocast was considered, with a final configuration of 11 landmarks (see Fig. 6). Shape variables were regressed onto centroid size, defined as the square root of the sum of squared distances of a set of landmarks from their centroid (22). PC analysis, centroid size, and multivariate regression were computed by APPLIED PROCRUSTES SOFTWARE (version 2.3, www.cpod.com/monoweb/aps). For overviews on the rationale of geometric morphometrics applied here, see in particular Rohlf and Bookstein (24), and Marcus *et al.* (22, 25).

Results

Metrics. The metric variables were processed to extract the first two PCs (Fig. 1a), which explain 74% and 14%, respectively, of the total variance. PC1 represents a general size vector, where all the variables show high positive loadings (>0.75 , except PC = 0.63). The height variables are those that are more correlated to this vector, with loadings up to 0.9. This axis distributes the sample according to the endocranial size, with a continuous increase from the smallest archaic specimens (SNG2, SAL, ZKD3, and TRN2) to the more encephalized Neandertals and modern humans. PC2 is mainly related to the parietal chord length, showing a loading of 0.71. The other variables do not show any remarkable correlation (loadings between -0.39 and $+0.36$). This second component, considered together with PC1, sorts the modern from the nonmodern sample. In both these groups, the more the size increases the more the parietal chord shortens. The archaic and Neandertal specimens fit a common size-related trajectory. In contrast, the modern group departs from this distribution by means of its parietal sagittal development. The inverse relation between size and parietal lengthening seems to be reproduced within the modern variability, but the small sample size does not allow a robust statistical approach. Considering the nonmodern trajectory, it should be noted that the SH4/5 endocasts exactly fit this pattern, and SCP1 shows only a slight departure.

Sorting the specimens by Euclidean distances and using the unweighted pair-group method using arithmetic averages cluster procedure (Fig. 1b), the three groups (i.e., ARC, NDR, and MOD) are classified appropriately by this endocranial morphometric analysis. We note the only exceptions represented by the SCP1 and SH4 endocasts, which group within the ARC and NDR samples, respectively, thus “inverting” their expected positions. The archaic cluster, in turn, is characterized by the distinction between smaller and larger (including SCP1) specimens. When the relative values are considered (Fig. 1c), the differences between modern and nonmodern specimens are more pronounced, whereas the archaic and Neandertal samples are less separated and SCP1 is grouped more appropriately. Interestingly, the Asian specimens (including the Arago endocast, the position of which seems biased by the specimens used in its reconstruction) cluster together. The recent human specimen (RHE) is set apart as an outlier of the modern group or of the entire sample, respectively, in the two analyses.

Geometric Morphometrics. By using the reduced configuration of landmarks, the 3D coordinates have been superimposed following the Procrustes procedure. The first two PCs of shape variation are considered here (Fig. 2a). PC1 explains 36% of the total variance, basically involving a decrease of the posterior (temporo-occipital) width compared with the anterior one (frontal), associated with vault heightening due to anterior development of the parietal chord (Fig. 2b). This component increases gradually from one group to another [i.e., moving from archaic (ARC) toward Neandertals (NDR) and up to modern (MOD) specimens], and it is slightly correlated with centroid size ($R^2 =$

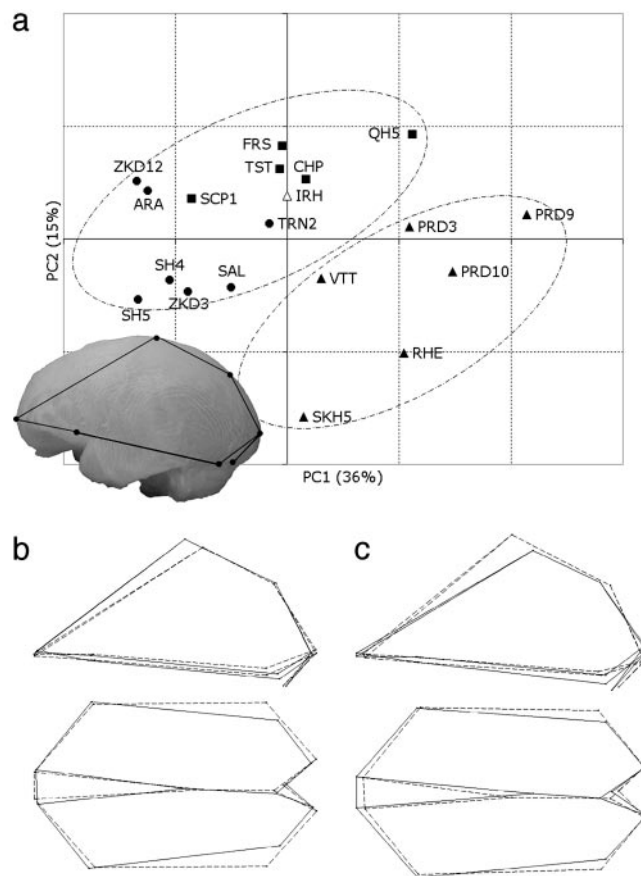


Fig. 2. Results of the PC analysis computed on the 11-landmark configuration (see Fig. 6) superimposed by the Procrustes procedure. (a) PC1 vs. PC2 (total variance explained = 51%). (b) Shape changes along the PC1 in left lateral (*Upper*) and superior views. (c) Shape changes along the PC2 in left lateral and superior views. Note the configuration in the left lateral view superimposed on the stereolithography of the SCP1 endocast. Solid and dashed links show the shifting of the configuration toward positive and negative values, respectively, of the morphological vectors.

0.48; $P < 0.001$). When PC2 (15% of the total variance) is also considered, the modern and nonmodern groups are separated. This second component involves a decrease of the posterior width compared with the anterior one (as described for the first axis), but with a general vault flattening that is mostly related to parietosagittal shortening (Fig. 2c). When these two components are considered together, the results previously obtained with traditional morphometrics are supported further and, in particular, better described as a 3D shape variation. As size increases, the frontal lobes widen with respect to the posterior areas. In addition, as size increases, the parietal chord shortens, or at the least it does not keep pace with the general enlargement. Eventually, the modern and nonmodern trajectories are separated by these two components because of the parietal development and vertical growth in the former group. In this general framework, the SH4/5 and SCP1 endocasts lie within the archaic variability.

A morphological synthesis of the pattern observed can be visualized by using the pairwise comparisons between average shapes, considering the entire endocranial morphology. The comparison between the archaic and Neandertal samples (Fig. 3a) shows slight vertical development, occipital reduction, and frontal development. In contrast, when the archaic and modern samples are compared (Fig. 3b), the outstanding differences are represented by an extreme vertical development, which seems to

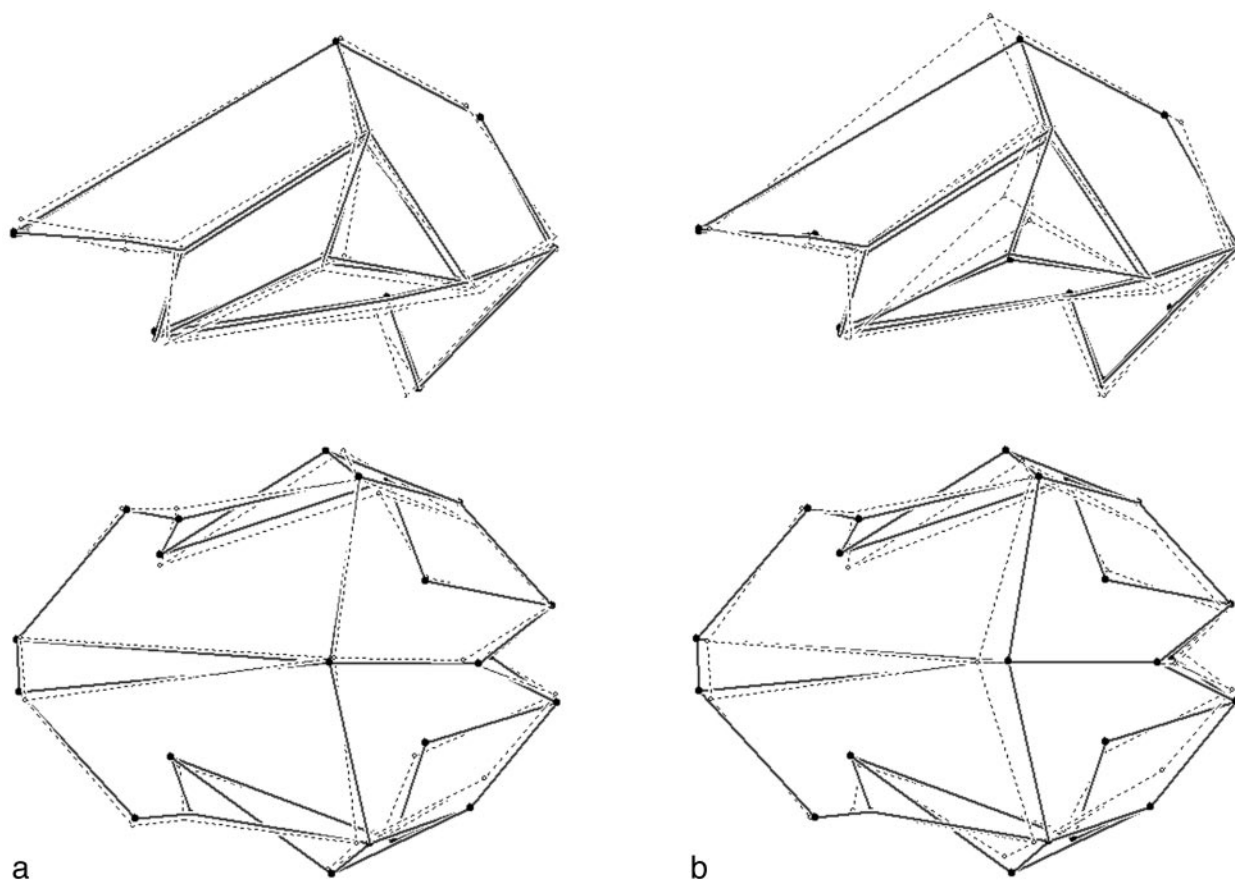


Fig. 3. Pairwise comparison between 23-landmark averaged configurations. (a) Archaic vs. Neandertal. (b) Archaic vs. modern (solid links, archaic average configuration; dashed links, Neandertal and modern average configuration).

be led by parietal growth and related to reduction of both the occipital areas and posterior basal widths.

Discussion

The tight structural relationship between brain and cranial development (8, 26) allows the study of cerebral surfaces directly by comparing endocranial structures. However, the correspondence between soft and hard tissues is not complete, and some caution must be used when hypotheses on brain morphology are based on endocranial anatomy (27, 28). In addition, the endocast morphology is elusive, many details are not easy to identify, and fossil specimens are usually fragmentary. These factors represent a severe limitation for any paleoneurological approach.

Even when these limits are taken into account, the multivariate analyses performed here show that a quantification of the general trends of endocranial shape variation in the genus *Homo* is possible. The main result was the identification of two different evolutionary trajectories, for which a similar expansion in endocranial size has been reached by different changes in shape.

We observed that archaic and Neandertal specimens share a common endocranial model, in which a large amount of variation is based on a single allometric trend. In this case, encephalization (viewed as cerebral volumetric expansion) structurally influences the variation in endocranial shape. This trajectory represents therefore a continuous gradation, ranging from archaic small specimens (i.e., Salè and the smallest Asian *H. erectus* fossils), to archaic larger ones (large-sized Asian *H. erectus* and European Middle Pleistocene specimens) up to the extremely encephalized Würmian Neandertals. This pattern mainly involves a relative reduction of the length and width of the occipital

lobes, a vertical development, an enlargement of the frontal breadth, and the shortening of the parietal chord.

In comparison with the archaic-Neandertal pattern described above, the modern range of variability lies on a separate morphological trajectory (approximately aligned with the nonmodern one). The allometric pattern is similar to the previous one, but the trajectory is shifted toward a larger amount of parietal development. Clearly, the modern parietal enlargement secondarily affects the entire cerebral shape. Nevertheless, given that the first axis of variability is size-related, it must be assumed that there is a shared allometric component within the entire genus *Homo* that needs to be investigated further. This component is expressed mainly by a relative frontal widening and by a vertical development of the whole structure. Actually, a parietal development was hypothesized to have had a role also in the radiation of the early hominids by means of its visuospatial integrative potentialities (4). Therefore, additional attention should be focused on these cerebral districts because of their general importance and the manifold hypothetical role played during human evolution in general.

When size-related variations are evaluated as consequences of differential quantitative development, it must be argued that a certain level of “allometric stasis” has occurred during the evolution of the genus *Homo*. The exception is represented by the transition to the new endocranial structural pattern associated with the emergence of *H. sapiens*. In addition, as far as these relative values are concerned, the modern variability seems to be rather large compared with the nonmodern one. It is noteworthy that the only recent human endocast examined here lies at the end of the modern trajectory, or else it acts as an outlier when

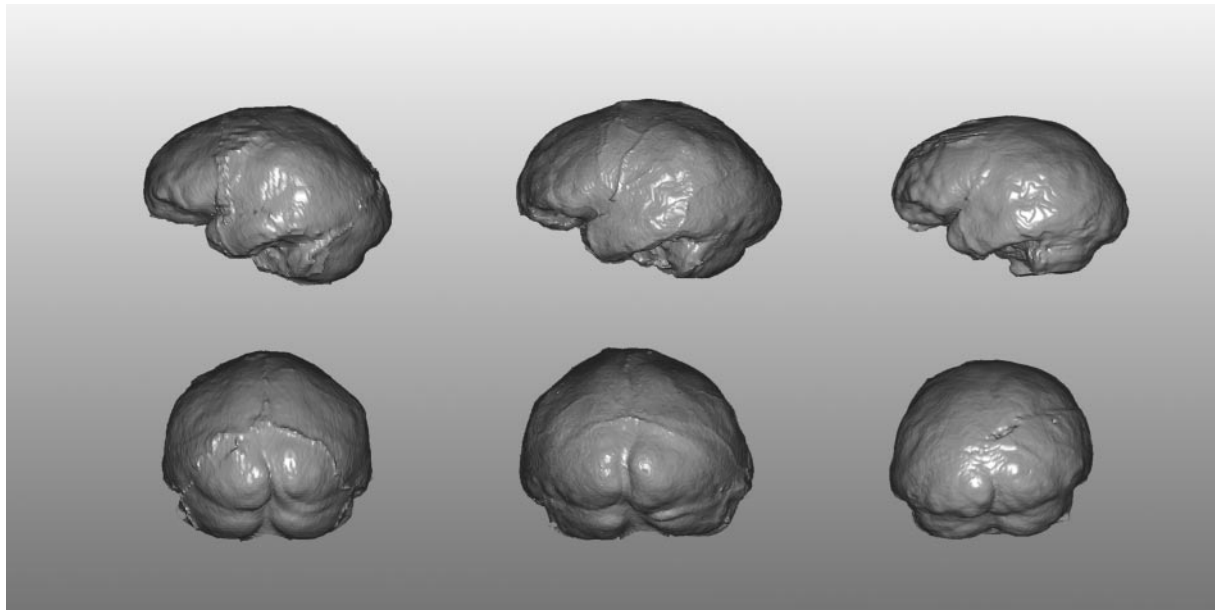


Fig. 4. Left lateral (*Upper*) and rear (*Lower*) views of the endocranial virtual reconstructions of Atapuerca SH5 (*Left*), Atapuerca SH4 (*Center*), and SCP1 (*Right*). The upper (parasagittal) parietal areas are flattened in the SH4/5 endocranials, with a consequent sloped and angled (tent-like) profile in posterior view. In contrast, the SCP1 endocranial shows a more rounded shape without any marked step parasagittally to the superior sagittal sinus.

the relative diameters are considered. This individual in fact shows a marked brachycephalic structure, which stresses the modern globularity of the brain. Anyhow, marked differences in endocranial shape between modern specimens of the Late Pleistocene and recent individuals has been noticed (9).

Thus, considering our sample as a whole, a large amount of the observed variability was achieved by a different expression of a common model and not by new structural relationships. Nevertheless, it can be hypothesized that also the nonmodern taxa may have undergone some minor specific process of differentiation, leading to the expression of peculiar features. The Asian *H. erectus* specimens show a marked occipital protrusion and deepening of confluence of sinuses that is not evident in either the later Neandertals or African specimens such as Salè nor is it evident, probably, in more archaic taxa such as WT-15000 (29). Even along the European sequence represented by the two chronospecies *Homo heidelbergensis* and *H. neanderthalensis*, some endocranial features probably represent late apomorphies. The specimens we examined here from the Sima de los Huesos, Saccopastore, and other European sites are especially appropriate for examining the evolution of the typical Neandertal morphology of the last glaciation and represent a useful case study to investigate the occurrence in human brain evolution of a continuum of variation vs. more discrete events. In accordance with the ectocranial evidence (13, 30, 31), the SH4/5 and SCP1 endocranials are somewhat intermediate along this hypothetical lineage, clustering with either the archaic or Neandertal morphotypes depending on the variables considered (raw vs. size-adjusted data). Nevertheless, if we look at the posterior view of both the SH4 and SH5 endocranials compared with that of SCP1 (Fig. 4), the two Spanish Middle Pleistocene specimens show a plesiomorphic “tent-like” profile (i.e., a parasagittal flattening), whereas the early Late Pleistocene specimen from Italy displays the development of the upper parietal gyrus observed in the Würmian Neandertals, with a consequent, more rounded profile in rear view. It therefore must be assumed that the major allometric trends in cephalic expansion do not exclude some minor but relevant structural rearrangements, apparently associated with a chronomorphological continuum.

We should note that, since the recovery of the Feldhofer calotte in 1856, a number of workers hypothesized that a comparable cranial capacity shared by modern humans and Neandertals may imply that the two morphotypes belonged to different lineages (32, 33). In fact, whether encephalization is interpreted as a progressive process (and, at the same time, similar endocranial volumes and a penecontemporaneous chronology are assumed for both the human morphs), the occurrence of distinct lineages is highly probable. Such a conclusion, apparently rather intuitive, required more than a century to be tested on the grounds of various sources of data and to find widespread acceptance among the scientific community (e.g., refs. 34–41). Accordingly, our data suggest that Neandertals and modern humans represent two distinct and independent evolutionary trajectories, in which the encephalization processes may have followed completely independent patterns despite the occurrence of similar selective pressures and autocatalytic evolutionary mechanisms. Thus, these two late human morphotypes represent the result of different biological models and are sustained by distinct ontogenetic pathways (42, 43) independent from their interbreeding potentialities. It must be stressed that, when also considering the ectocranial counterpart in multivariate and landmark-based approaches, the neural globularity has been described as a discrete modern human phenotypic character (32) or even a modern human autapomorphy (44).

Considering the allometric pattern described here, it may be assumed that some structural boundaries were reached by the expansion of cerebral surfaces (e.g., the parietal areas) during the late evolution of the genus *Homo*. It is conceivable that this functional matrix may have involved some biomechanical stress and troubles in the ossification process of the cranium. This observation is consistent with the evidence of some level of “ontogenetic stress” registered by the high occurrence of hypostotic discrete traits in the posteriolateral districts of the cranial vault, unexpectedly observed among Neandertal and European Middle Pleistocene samples (23, 46). The parietal development of the modern morphotype may have represented a key to surpass the encephalization constraints imposed by the archaic structural model. It is reasonable to assume that this morpho-

logical discrete reassessment could have been matched to some level of neurological reconfiguration.

A number of people were of great help in the development of this work. We especially thank Marie-Antoinette and Henry de Lumley for kindly allowing the analysis of the endocast collection preserved at the Institute de Paléontologie Humaine (Paris). Dominique Grimaud-Hervé was a funda-

mental reference of E.B. during a brief stage in Paris. We also thank Leslie Aiello, Dean Falk, and Dennis Slice for useful comments and suggestions. We are grateful to colleagues in our respective institutions for support and encouragement, with a special mention to Ana Gracia, Patricio Dominguez, Carlos Lorenzo, and Pietro Passarello. Rolf Quam kindly reviewed our Mediterranean English. This work was partly supported by the Italian Ministero dell' Istruzione, dell' Università e della Ricerca (including Cofin grants).

1. Tobias, P. V. (1971) *The Brain in Hominid Evolution* (Columbia Univ. Press, New York).
2. Godfrey, L. & Jacobs, K. H. (1981) *J. Hum. Evol.* **10**, 255–272.
3. Falk, D. (1987) *Annu. Rev. Anthropol.* **16**, 13–30.
4. Holloway, R. L. (1995) in *Origins of the Human Brain*, eds. Changeaux, J. P. & Chavaillon, J. (Clarendon, Oxford), pp. 42–54.
5. Ruff, C. B., Trinkaus, E. & Holliday, T. W. (1997) *Nature* **387**, 173–176.
6. Conroy, G., Weber, G., Seidler, H., Recheis, W., Zur Nedden, D. & Mariam, J. H. (2000) *Am. J. Phys. Anthropol.* **113**, 111–118.
7. Falk, D. (1986) in *Comparative Primate Biology Vol. 1: Systematics, Evolution, and Anatomy*, eds. Swindler, D. R. & Erwin, J. (Liss, New York), pp. 477–490.
8. Moss, M. L. & Young, R. W. (1960) *Am. J. Phys. Anthropol.* **18**, 281–292.
9. Grimaud-Hervé, D. (1997) *L'Évolution de l'Enchéphale chez Homo erectus et Homo sapiens* (Centre National de la Recherche Scientifique, Paris).
10. Rohlf, F. J. & Marcus, L. F. (1993) *Trends Ecol. Evol.* **8**, 129–132.
11. Bischoff, J. L., Shampa, D. D., Aramburu, A., Arsuaga, J. L., Carbonell, E. & Bermúdez de Castro, J. M. (2003) *J. Archaeol. Sci.* **30**, 275–280.
12. Arsuaga, J. L., Martínez, I., Gracia, A., Carretero, J. M. & Carbonell, E. (1993) *Nature* **362**, 534–537.
13. Arsuaga, J. L., Martínez, I., Gracia, A. & Lorenzo, C. (1997) *J. Hum. Evol.* **33**, 219–281.
14. Manzi, G., Bruner, E., Caprasecca, S., Gualdi, G. & Passarello, P. (2001) *Riv. Antropol.* **79**, 61–72.
15. Bruner, E., Manzi, G. & Passarello, P. (2002) in *Three-Dimensional Imaging in Paleoanthropology and Prehistoric Archaeology*, British Archeol. Records IS 1049, eds. Mafart, B. & Delingette, H. (Archeopress, Oxford), pp. 17–24.
16. Zollikofer, C. P. E., Ponce de León, M. S. & Martin, R. D. (1998) *Evol. Anthropol.* **6**, 41–54.
17. Tobias, P. V. (2001) *Clin. Anat.* **14**, 134–141.
18. Felsenstein, J. (1989) *Cladistics* **5**, 164–166.
19. Page, R. D. M. (1996) *Comput. Appl. Biosci.* **12**, 357–358.
20. Slice, D. (2000) MORPHEUS ET AL. (State University of New York, Stony Brook).
21. Valeri, C. J., Cole, T. M., 3rd, Lele, S. & Richtsmeier, J. T. (1998) *Am. J. Phys. Anthropol.* **107**, 113–124.
22. Marcus, L. F., Corti, M., Loy, A., Naylor, G. J. P. & Slice, D. E. (1996) *Advances in Morphometrics* (Plenum, New York).
23. de Lumley, H., de Lumley, M. A. & David, R. (1982) in *Préirage du 1er Congrès International de Paléontologie Humaine* (Nice, October 1982) (Centre National de la Recherche Scientifique, Paris), Tome 1, plates 9–17.
24. Rohlf, F. J. & Bookstein, F. L. (1990) *Proceedings of the Michigan Morphometrics Workshop* (Univ. of Michigan Museum of Zoology, Ann Arbor).
25. Marcus, L. F., Bello, E. & Garcia-Valdecasas, A. (1993) *Contribution To Morphometrics* (Museo Nacional de Ciencias Naturales, Madrid).
26. Enlow, D. H. (1990) *Facial Growth* (Saunders, Philadelphia).
27. Kimbel, W. H. (1984) *Am. J. Phys. Anthropol.* **63**, 243–263.
28. Peña-Melian, A. (2000) *Hum. Evol.* **15**, 99–112.
29. Begun, D. & Walker, A. (1993) in *The Nariokotome Homo erectus Skeleton*, eds. Walker, A. & Leakey, R. (Springer, Berlin), pp. 326–358.
30. Martínez, I. & Arsuaga, J. L. (1997) *J. Hum. Evol.* **33**, 283–318.
31. Manzi, G., Saracino, B., Bruner, E. & Passarello, P. (2000) *Riv. Antropol.* **78**, 193–204.
32. Huxley, T. H. (1863) *Evidence as to Man's Place in Nature* (D. Appleton, New York).
33. King W. (1864) *Q. J. Sci.* **1**, 88–97.
34. Stringer, C. B. & Andrews, P. (1988) *Science* **239**, 1263–1268.
35. Stringer, C. B. (1994) in *Origins of Anatomically Modern Humans*, eds. Nitecki, M. H. & Nitecki, D. V. (Plenum, New York), pp. 149–172.
36. Rak, Y. (1993) in *Species, Species Concepts, and Primate Evolution*, eds. Kimbel, W. H. & Martin, L. B. (Plenum, New York), pp. 523–536.
37. Waddle, D. M. (1994) *Nature* **368**, 452–454.
38. Hublin, J. J., Spoor, F., Braun, M., Zonneveld, F. & Condemi, S. (1996) *Nature* **381**, 224–226.
39. Turbon, D., Pérez-Pérez, A. & Stringer, C. B. (1997) *J. Hum. Evol.* **32**, 449–468.
40. Krings, M., Capelli, C., Tschentscher, F., Geister, H., Meyer, S., von Haeseler, A., Grossschmidt, K., Possnert, G., Paunovic, M. & Paabo, S. (2000) *Nat. Genet.* **26**, 144–146.
41. Harvati, K. (2003) *J. Hum. Evol.* **44**, 107–132.
42. Dean, M. C., Stringer, C. B. & Bromage, T. G. (1986) *Am. J. Phys. Anthropol.* **70**, 301–309.
43. Ponce de León, M. S. & Zollikofer, C. P. E. (2001) *Nature* **412**, 534–538.
44. Lieberman, D. E., McBratney, B. M. & Krovits, G. (2002) *Proc. Natl. Acad. Sci. USA* **99**, 1134–1139.
45. Manzi, G., Vienna, A. & Hauser, G. (1996) *J. Hum. Evol.* **30**, 511–527.
46. Manzi, G., Gracia, A. & Arsuaga, J. L. (2000) *J. Hum. Evol.* **38**, 425–446.